IEEE Access
Multidisciplinary ⋮ Rapid Review ⋮ Open Access Journal

Received April 22, 2020, accepted May 26, 2020, date of publication June 8, 2020, date of current version June 18, 2020.

Digital Object Identifier 10.1109/ACCESS.2020.3000533

Modeling of Tire Vertical Behavior Using a Test Bench

ENRIQUE CARABIAS ACOSTA, JUAN J. CASTILLO AGUILAR, (Member, IEEE), JUAN A. CABRERA CARRILLO, JUAN M. VELASCO GARCÍA, (Student Member, IEEE), JAVIER PÉREZ FERNÁNDEZ, (Graduate Student Member, IEEE), AND MANUEL G. ALCÁZAR VARGAS, (Student Member, IEEE)

Department of Mechanical Engineering, University of Malaga, 29071 Málaga, Spain

Corresponding author: Juan J. Castillo Aguilar (juancas@uma.es)

This work was supported in part by the Ministry of Economy, Industry and Competitiveness under Grant TRA2015-67920-R, and in part by the University of Malaga.

ABSTRACT Tire models are of great importance for precise investigations of vertical vehicle dynamics, including vehicular safety and riding comfort. An adequate modeling of the tire is crucial to properly reproduce vehicle vertical behavior in simulations and to evaluate the influence of the tire in the overall performance of the suspension system. This paper introduced vehicle single-point tire models and, thereafter, investigated the influence of the excitation frequency and inflation pressure on the damping and stiffness coefficients of the proposed tires experimentally. In this manner, a test-bench was used to obtain the model parameters of a light vehicle tire and a motorcycle tire. Given the obtained results, it has been observed that both factors have a significant effect on the parameters of the proposed tire models. Moreover, a quarter car suspension model was investigated using the modelled tires to illustrate the influence of the correct characterization of the tire on the vertical suspension performance.

INDEX TERMS Automotive testing, hysteresis, road vehicles, single point models, tire models, vehicle vertical dynamics, viscoelasticity.

I. INTRODUCTION

The proper modeling of the tire is essential to adequately reproduce vehicle vertical behavior in vehicle dynamics simulations. The study of the characteristics of the tire is complex due to its geometry, the great deformation it suffers and the diversity of materials of which it is composed. For this reason, many research groups devote great effort in developing models that make it possible to reproduce tire forces and moments [1]–[4]. Vehicle vertical dynamics is mainly determined by the suspension system and the tire. Good vehicle vertical behavior is desirable because it will not only improve the comfort of the occupants, but it will also contribute to a better performance of the vehicle in traction and braking processes. To this end, the use of accurate vertical tire models is decisive.

Most research papers related to suspension systems and vehicle vertical dynamics resort to single point contact tire models using lumped parameters. In the well-known Kelvin-Voigt model [5], the tire is simply modelled using a spring with constant stiffness or, at best, using a spring and a damper connected in parallel, also with constant stiffness and damping coefficients. However, this model does not reproduce the viscoelastic behavior of the tire and does not accurately represent the physics of the contact between the tire and the road. A model that takes into account the viscoelastic behavior of the tire is the Maxwell model [5], [6]. Other authors studied the influence of hysteresis on both the longitudinal and vertical modeling of tires [7], [8]. There are also tire models based on the 'flexible ring theory' that characterize their frequency response [9]–[12]. Finally, some researches focus on the characterization of the frequency behavior of the tire through experimental tire modal parameters to calculate the static vertical tire stiffness on both drum and flat road surfaces and the distribution of vertical and shear forces [13], [14]. Interestingly, due to the importance of the tire in the improvement of driver comfort in most agricultural wheeled tractors, which commonly lack a suspension system,

The associate editor coordinating the review of this manuscript and approving it for publication was Jianyong Yao.

several studies model the vertical behavior of the tire and determine which factors influence tire stiffness and damping coefficients [15], [16].

All these models need to obtain the characteristic stiffness and damping coefficient through tire bench tests.

There are different methods to measure tire stiffness and damping coefficient. According to the proposed methodology, they can be grouped as follows [9], [16]:

- Static load-deflection. Static stiffness of a non-rotating tire on a drum or flat road surface by increasing the static load and measuring the static loaded radius.
- Non-rolling vertical free vibration. Dynamic stiffness of a tire by dropping the tire from a known height and obtaining the vertical position versus time data.
- Non-rolling equilibrium load-deflection. Dynamic stiffness of a non-rotating tire on a drum or flat road surface by applying a vibration or variable displacement and measuring the dynamic loaded radius.
- Rolling vertical free vibration. The method is a vertical free vibration but applied to a rolling tire.
- Rolling equilibrium load-deflection. Dynamic stiffness of a rotating tire on a drum or flat road surface by applying a variable displacement.

In some cases, test benches used to determine tire vertical stiffness and damping do not only take into account the deformation of the tire, but are also influenced by the deformation of the rim and by the effects of the unsprung mass. This situation is commonly found in test benches in which the tire is rotating. To solve this problem, a test bench in which only the tire is taken into account in the measurement of stiffness and damping coefficients has been developed in this work. Besides, this test bench makes it possible to study other effects such as tire viscoelasticity and hysteresis. Consequently, this bench allows obtaining tire parameters and more accurate single point contact models as well as studying the factors that influence on the value of these parameters.

In this paper, the proposed test bench has been used for the modeling of two tires of size 205/65 R15 and 90/58 R17. The first is a tire commonly used in light four-wheeled vehicles while the second is designed to be used in motorcycles. Data obtained from tests are used to fit single point contact tire model parameters. Thus, tire stiffness and damping, viscoelastic behavior and hysteresis are determined. Furthermore, the influence of the excitation frequency and inflation pressure is evaluated. It has been found that there is a considerable difference between the parameters obtained for both the motorcycle tire and for the vehicle. These results are of great interest, since there is not much information about the modeling of motorcycle tires in literature. This way, this work will contribute to improving motorcycle dynamics models and the safety of this type of vehicles. The main contributions of this paper are the following:

- to evaluate the influence of excitation frequency and inflation pressure on the damping and stiffness coefficients of single point tire models.

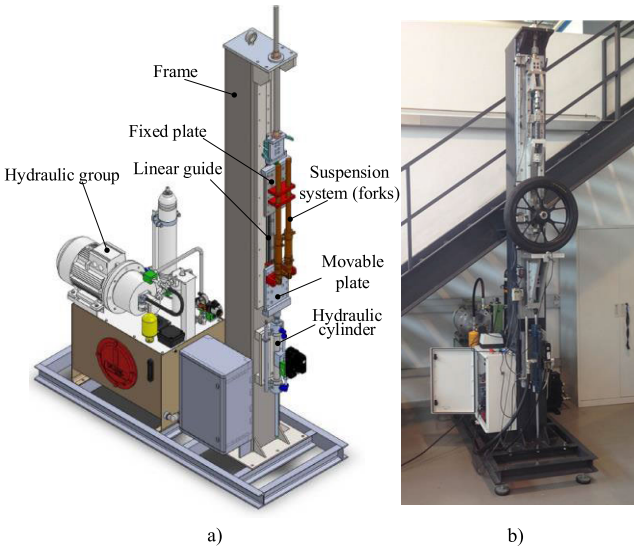

FIGURE 1. Tire and suspension system test bench. (a) 3D-model (b) Photograph.

- to study the influence of modeling of the tire on the vertical suspension performance.

This paper is organized as follows: the test bench developed to obtain the vertical behavior of tires is described in section II. In section III, single point contact models used to reproduce tire behavior are explained. Section IV is devoted to describing the experimental tests carried out and the methodology proposed to obtain tire model parameters. Tire model parameters obtained from tests conducted with the aforementioned tire are also included. The influence of the models obtained in the previous section on vehicle vertical dynamics is evaluated in section V. Finally, conclusions are drawn in section VI.

II. TEST BENCH

To carry out this work, a test bench designed by this research team was built. This test bench makes it possible to study and characterize the vertical behavior of tires and vehicle suspension systems and components (see Figure 1). Thus, this versatile test bench can be used to model the behavior of two- and four-wheeled vehicle suspensions. The shock absorber and the spring response can be tested independently or, if necessary, the whole suspension system can be tested simultaneously. Furthermore, the tire response can also be studied independently by fixing the tire to the structure of the test bench and applying a displacement of controlled frequency and amplitude. To remove the influence of rim deformation, the deformation of the rim where the tire is mounted is measured with a sensor and the different displacements are normalized to obtain the tire deformation. This way, only the tire response is measured and modelled.

The bench is composed of a frame, which must withstand the forces and vibrations transmitted by the tested elements. These efforts are transmitted to the bench through a linear guide, where a fixed and a mobile plate are connected.

TABLE 1. Test bench general technical characteristics.

Parameter	Value
Maximum measurable force (Traction -compression)	±10 kN
Testing speed	from 0.05 mm/s to 2.1 m/s with continuous variation
Maximum cylinder rod stroke	350 mm
Test frequency range	0 to 25 Hz with continuous variation
Control loop frequency	1 kHz
Maximum data recording frequency	10 kHz
DAQ resolution	Up to 24 bits

TABLE 2. Measurement system.

Number, sensor type and model	Accuracy	Measurement principle	Range
1 x displacement sensor Schreiber SM42	±0.05 mm	Inductive - LVDT	0-360 mm
2 x displacement sensor OMRON ZX-LD40	±2 µm	Laser	30-60 mm
2 x displacement sensor OMRON ZX-LD100	±16 µm	Laser	60-140 mm
1 x Load cell HBM U93 10kN	±1 N	Strain gauge	±10 kN
1 x Load cell Honeywell 125-100kg	±0.1 N	Strain gauge	±1kN
2 x accelerometer KYOWA AS-2G	±0.01 m/s^2	Piezo-resistive	±2 g
2 x accelerometer KYOWA AS-5G	±0.02 m/s^2	Piezo-resistive	±5 g
2 temperature sensors OPTRIS CS	±0.1°C	Infrared	-20°- 150°C

Depending on the type of test, the forces on the unsprung mass, the damping system or the tire will be transmitted and measured. The movable plate is the component that transmits the movement or vibration input to the system. In this work, the tire is mounted on a rim that is fixed to the bedplate.

The excitation to the parts to be tested is generated by a hydraulic cylinder controlled by a servo-valve. This way, a controlled displacement or force is transmitted to the plate where the tire is placed. The control system makes it possible to simulate different types of inputs, such as sinusoidal, ramp, bump and random. The characteristics of the test bench are summarized in Table 1. The measurement system installed in the test bench is described in Table 2.

The control of the test bench is carried out by an algorithm programmed in a CompactRio-9066®real time system. Input and output modules are connected to an FPGA. Real time loop communicates with the FPGA to perform data transmission and to establish the desired control action (see Figure. 2).

III. TIRE VERTICAL MODELING

There are numerous mathematical models described in literature [5], [17], [18] to model the hysteresis and viscoelastic behavior of materials and components. Among them, some of the most widely used models in the case of tires are the so-called 'single point contact models'. In these models, the entire part of the tire in contact with the road is reduced to a single point contact, so that neither the length nor the contact area is taken into account. These models are composed of a combination of ideal elastic elements (springs) and energy dissipators (dampers). Their main field of application is related to modeling the behavior of suspension systems and the vertical dynamics of vehicles. In this work, the vertical behavior of the tire is modeled with three different single point contact model approaches (see Figure 3).

The first one is a Kelvin-Voigt model in which a damper element and two spring elements [5], [17] are included (Figure 3a). All components are arranged in parallel. The first spring (K_s) represents the static stiffness of the tire. The second spring (K_d) is used to model the change in stiffness with the frequency of the excitation [14]. The damper (C_d) allows evaluating the damping of the tire and its variation with the frequency of the excitation (ω). The basic equation for this model is the following:

$$F = C_d \cdot (\dot{x}_t - \dot{x}_r) + K_d(\omega) \cdot (x_t - x_r - \delta) + K_s \cdot (x_t - x_r) \quad (1)$$

where F is the total force provided by each model, $(x_t - x_r)$ is the tire displacement (x_t being equal to zero in our test) and δ is the initial displacement.

The second model is composed of a Maxwell model in parallel with a spring element [5], [17]. This model is also called Standard Linear Model (Figure 3b). This model is governed by the following equations:

$$F = K_s \cdot (x_t - x_r) + f_v \quad (2)$$

$$\dot{f}_v + \frac{K_d}{C_d} \cdot f_v = (\dot{x}_t - \dot{x}_r) \quad (3)$$

where f_v represents the viscoelastic force.

Finally, the third model is the simple Bouc model [18]. This model is similar to the Kelvin-Voigt model, but incorporates a fourth element that reproduces the hysteresis of the material (Figure 3c). The equations that describe this model are:

$$F = C_d \cdot (\dot{x}_t - \dot{x}_r) + K_d(\omega) \cdot (x_t - x_r - \delta) + K_s \cdot (x_t - x_r) + \alpha \cdot z \quad (4)$$

$$\dot{z} = A \cdot (\dot{x}_t - \dot{x}_r) + \mu \cdot (\dot{x}_t - \dot{x}_r) \cdot |z|^n - \gamma \cdot |\dot{x}_t - \dot{x}_r| \cdot |z|^{n-1} \quad (5)$$

where z is an auxiliary term that models the hysteresis by means of parameters A, μ and γ and α is a scaling factor.

Once the equations that determine the force in the tire for the three proposed models have been obtained, data obtained in the bench can be used to obtain the fundamental parameters of each model, such as the static stiffness (K_s), dynamic stiffness (K_d) and dynamic damping (C_d) coefficients.

The main reason why these parameters and models were chosen to represent the vertical behavior of the tire was derived from the observation of Figure 4a. In the first place, this figure shows the static stiffness of the tire that was measured by conducting tests at very low speed and measuring the vertical force. The tests included the data measured during the loading and unloading processes. Next, the vertical forces that were measured in dynamic tests at different excitation

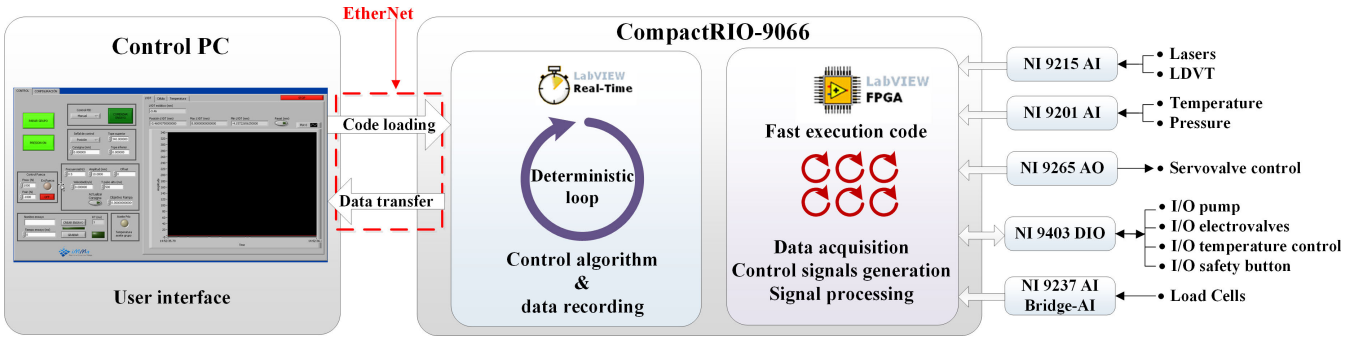

FIGURE 2. Scheme of the test bench control system.

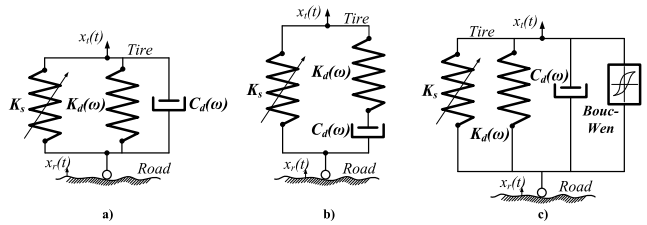

FIGURE 3. Single point contact tire vertical models. (a) Kelvin-Voigt (b) Maxwell (c) Bouc.

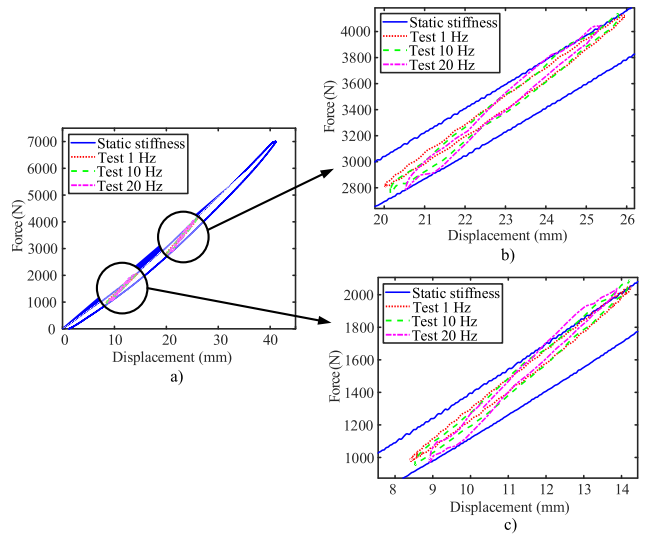

FIGURE 4. Tire forces measured at 1, 10 and 20 Hz vs displacement. (a) Static and dynamic stiffness (b) Preload 3500 N (c) Preload 1500 N.

frequencies (1, 10 and 20 Hz) are also included in the figures. Two series of tests were conducted with 3500 N and 1500 N of preload in the tire (Figures 4b and 4c respectively). A local increase of the stiffness in both series of tests can be observed, i.e., the static stiffness curve has a lower slope compared to the dynamic stiffness. Furthermore, the higher the excitation frequency, the higher the increase in the slope of the dynamic stiffness. For this reason, the static and dynamic stiffness has been modelled separately in each of the previous models. Dynamic damping has also been modelled to obtain the energy dissipation behavior of the tire as a function of the excitation frequency.

IV. TESTS

The goal of these tests was to evaluate the influence of the frequency of the excitation and the inflation pressure on the parameters of tire single point contact models. A light vehicle and a motorcycle tires were used in this series of tests. First, the static stiffness was measured in a quasi-static test. Next, sinusoidal movements of frequency between 1 and 20 Hz were reproduced. Amplitudes of 3 and 2 mm were programmed for the light vehicle and the motorcycle tire respectively. As described before, control was performed with a real time system. The control system loop frequency and data acquisition sampling rate were fixed at 1000 Hz. Actual bedplate displacement and rim deformation were measured using a high accuracy linear variable differential transducer and a laser displacement sensor respectively. Forces were measured using a load cell located in the fixed plate. An optimization algorithm provided the parameters that best fit the tire model output to the experimental data. Finally, results were analyzed and interpreted.

As mentioned before, static rigidity (K_s) was obtained through an experimental test in which the tire was deformed progressively from zero to maximum deflection (Figure 4). The vertical force was measured during this process. These data allowed obtaining the change of rigidity vs displacement of the tires.

Next, tests were carried out in which a sinusoidal movement was generated in the bedplate. Tests were conducted at different frequencies, amplitudes and preloads. This way, the change of parameters with the frequency was determined.

An algorithm based on Particle Swam optimization was used to perform parameter identification [19]. Data measured in the test bench were fitted to each model. The algorithm yielded the parameters that best modelled the experimental data. To do so, a goal function was defined. In this case, the average of the quadratic error between the measured force and the force provided with the model was selected as the goal function to be minimized. The following parameters were used in the optimization algorithm: number of particles per group = 30, number of groups = 2, number of iterations = 200, acceleration factors = 0.49445 and initial and final weights equal to 0.9 and 0.4 respectively. This way, two

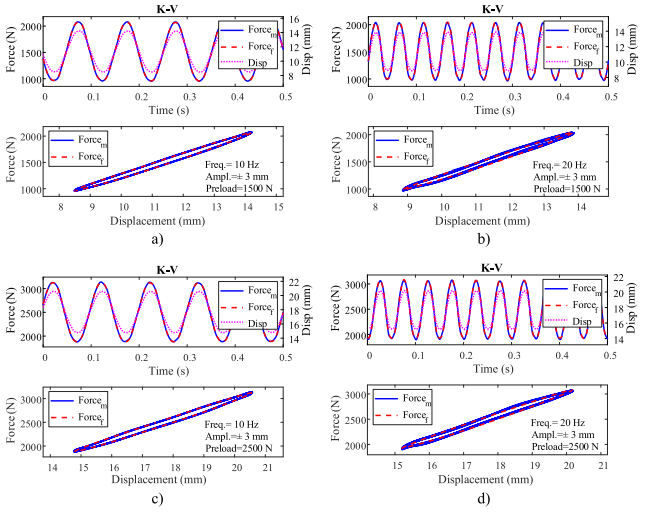

FIGURE 5. Test data fitting using the Kelvin-Voigt model. (a) Frequency 10 Hz, preload 1500 N (b) Frequency 20 Hz, preload 1500 N (c) Frequency 10 Hz, preload 2500 N (d) Frequency 20 Hz, preload 2500 N.

(K_d, C_d) or six (K_d, C_d, α, A, μ, γ) additional parameters were obtained to model the vertical behavior of the tire.

A. TESTS WITH A TIRE OF SIZE 205/65 R15

First, tests were conducted using a 205/65 R15 tire. This tire size is commonly used in light passenger cars. An amplitude of 3 mm was set in these tests. Test frequencies were 1, 5, 10, 15 and 20 Hz. Finally, three preload conditions were simulated, 1500, 2500 and 2500 N. In these tests, inflation pressure (P_n) was set at 1.8 bar.

1) KELVIN-VOIGT MODEL

The following plots show the results obtained at two frequencies, 10 and 20 Hz, with two preloads, 1500 and 2500 N (Figure 5) using the Kelvin-Voigt model. Model parameters were obtained by means of the aforementioned optimization algorithm. Two plots are generated with each test. The first one includes the force measured (Force_m), the force provided by the fitted model (Force_f) and the displacement (Disp) plotted vs time. In addition, the second plot includes the measured and the fitted forces plotted vs the displacement.

It can be seen that the force provided by the model fits the measured force measured properly. Furthermore, the model reproduces the measured data adequately for all frequencies and preload conditions in the tire. Similar performance was observed for all tests. Finally, results using the Kelvin-Voigt model equation (eq. 1) for all tests are shown in Table 3.

Table 3 includes the test conditions, i.e. preload and excitation frequency, static rigidity and the model optimized parameters. Minimum error obtained after the optimization process is also included. For the sake of clarity, Figure 6 shows the evolution of the dynamic stiffness and damping coefficients as a function of the excitation frequency.

In this case, dynamic stiffness increased with the frequency of excitation whatever preload condition was imposed. On the other hand, dynamic damping decreased with frequency, being relatively high at low frequencies. However, low damping coefficients were observed for frequencies above 5 Hz.

TABLE 3. Summary of results using the Kelvin-Voigt model. Tire size: 205/65 R15. Inflation pressure = 1.8 bar.

Preload [N]	Frequency [Hz]	K_s [N/m]	K_d [N/m]	C_d [Ns/m]	Error [N^2]
1500	1	151227	31217	2224	7.03
1500	5	151227	38378	520	7.16
1500	10	151227	43796	283	22.04
1500	15	151227	49735	200	93.18
1500	20	151227	61042	150	220.85
2500	1	169325	30984	2534	16.24
2500	5	169325	38977	585	12.89
2500	10	169325	44483	320	52.32
2500	15	169325	51148	226	122.01
2500	20	169325	62415	170	269.14
3500	1	182145	36111	2826	28.53
3500	5	182145	45772	657	28.44
3500	10	182145	52015	362	65.50
3500	15	182145	59391	253	206.70
3500	20	182145	71370	184	400.38

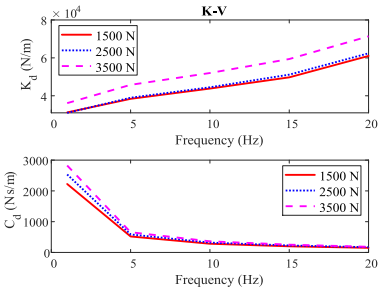

FIGURE 6. Stiffness and damping coefficients of the Kelvin-Voigt model vs excitation frequency. Tire 205/65 R15 (1.8 bar).

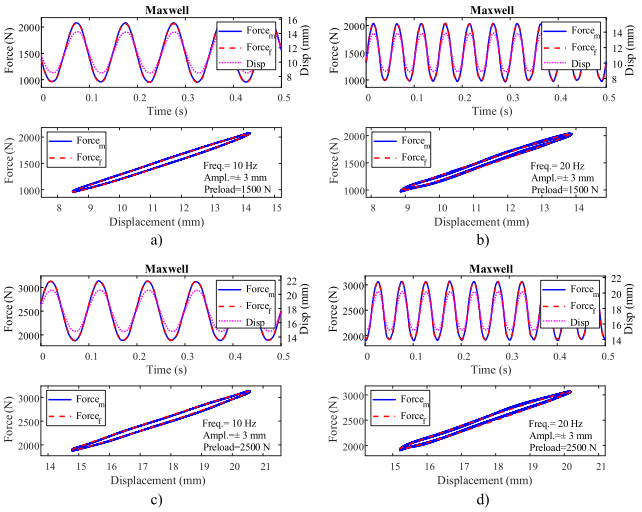

FIGURE 7. Test data fitting using the Maxwell model. (a) Frequency 10 Hz, preload 1500 N (b) Frequency 20 Hz, preload 1500 N (c) Frequency 10 Hz, preload 2500 N (d) Frequency 20 Hz, preload 2500 N.

2) MAXWELL MODEL

Similarly, the following plots show the results obtained at two frequencies, 10 and 20 Hz, with two preloads, 1500 and 2500 N using the Maxwell model (Figure 7). Plots show the

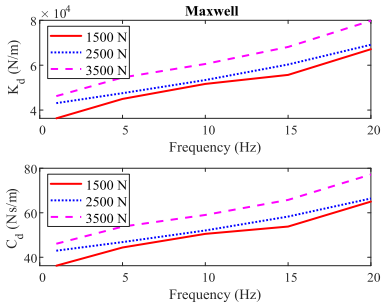

FIGURE 8. Stiffness and damping coefficients of the Maxwell model vs excitation frequency. Tire 205/65 R15 (1.8 bar).

TABLE 4. Summary of results using the Maxwell model. Tire size: 205/65 R15. Inflation pressure = 1.8 bar.

Preload [N]	Frequency [Hz]	K_s [N/m]	K_d [N/m]	C_d [Ns/m]	Error [N^2]
1500	1	151227	36302	36.20	106.92
1500	5	151227	44970	44.39	258.46
1500	10	151227	51654	50.52	182.16
1500	15	151227	55670	53.80	324.57
1500	20	151227	67131	65.02	181.65
2500	1	169325	43091	42.95	308.15
2500	5	169325	47528	46.82	200.58
2500	10	169325	53384	52.04	286.55
2500	15	169325	60311	58.29	289.03
2500	20	169325	69115	66.42	639.09
3500	1	182145	46217	46.07	244.67
3500	5	182145	54521	53.77	281.81
3500	10	182145	60549	59.02	213.08
3500	15	182145	68138	65.78	451.97
3500	20	182145	79822	77.21	404.01

data reproduced by the model according to equations (2) and (3) with the obtained optimized parameters.

As for the previous model, the fitting of test data with the model is suitable both for the case of frequency variation and when the preload is changed. Optimized parameters using the Maxwell model for all tests are shown in Table 4.

In the case of the Maxwell's model, it can be seen in Figure 8 and Table 4 that the dynamic stiffness values are of the same order of magnitude as those obtained in the previous model. On the contrary, the dynamic damping values are much smaller. It can also be observed that both stiffnesses and dynamic damping coefficients increase with the vibration frequency.

3) BOUC MODEL

This more complex model, which is commonly used for reproducing hysteresis, was also used. According to equations (4) and (5), the Bouc model requires the estimation of four additional parameters (α, A, γ and μ). Parameter n was set at 1. As a consequence, the computational time to obtain the estimation of the model parameters was considerably longer.

The following plots show the results obtained at two frequencies, 10 and 20 Hz with 2500 N of preload using the Bouc Model (Figure 9).

Optimized parameters using the Bouc model for all tests are shown in Table 5. Interestingly enough, errors are lower

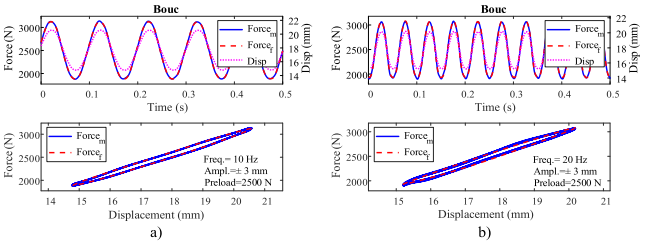

FIGURE 9. Test data fitting using the Bouc model. (a) Frequency 10 Hz (b) Frequency 20 Hz. Preload 2500 N.

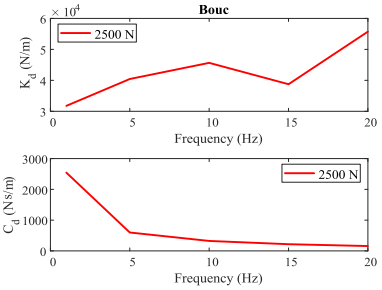

FIGURE 10. Stiffness and damping coefficients of the Bouc model vs excitation frequency. Tire 205/65 R15 (1.8 bar).

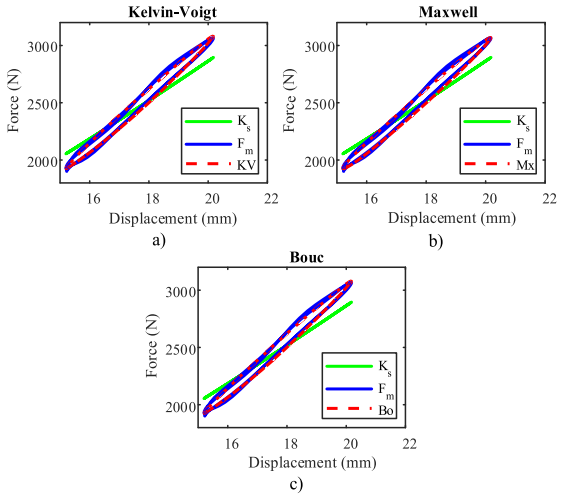

FIGURE 11. Comparison of three single point models. Tire 205/65 R15. (a) Kelvin-Voigt (b) Maxwell (c) Bouc.

compared to the other models. However, the improvement is small. Due to the higher computational cost that this model requires in the optimization process and during its use in simulations, this model is only recommended when the accuracy required in the simulations is very high.

Figure 10 shows the value of main parameters K_d and C_d provided by the model according to equations (4) and (5). Dynamic stiffness gradually increases with respect to frequency, except for the frequency of 15 Hz. Damping coefficients have similar behavior to the one obtained for the Kelvin-Voigt model.

4) MODELS COMPARATIVE

Once the results for the three single point models have been shown, a comparison of the three models used is shown

TABLE 5. Summary of results using the Bouc model. Tire size: 205/65 R15. Inflation pressure = 1.8 bar.

Preload [N]	Frequency [Hz]	K_s [N/m]	K_d [N/m]	C_d [Ns/m]	α	A	γ	μ	Error [N^2]
2500	1	169325	31750	2545	9	-11	60	1000	15.15
2500	5	169325	40438	598	-33	113	81	829	12.23
2500	10	169325	45652	324	51	-26	200	11	52.18
2500	15	169325	38757	218	237	103	38	671	108.22
2500	20	169325	55728	158	176	78	143	697	262.27

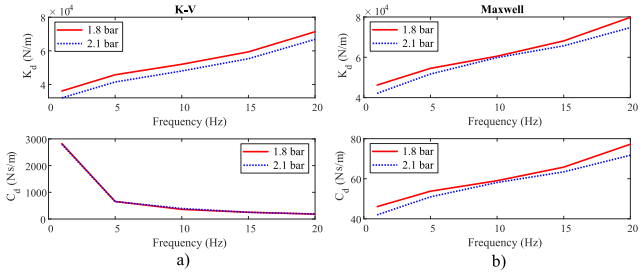

FIGURE 12. Comparison at different inflation pressures, 1.8 and 2.1 bar vs excitation frequency. (a) Kelvin-Voigt (b) Maxwell.

TABLE 6. Summary of results using the Kelvin-Voigt model. Tire size: 205/65 R15. Inflation pressures 1.8 and 2.1 bar.

		Inflation pressure 1.8 Bar.			Inflation pressure 2.1 Bar.		
Preload [N]	Frequency [Hz]	K_s [N/m]	K_d [N/m]	C_d [Ns/m]	K_s [N/m]	K_d [N/m]	C_d [Ns/m]
3500	1	182145	36111	2826	210282	32040	2797
3500	5	182145	45772	657	210282	41475	653
3500	10	182145	52015	362	210282	48035	394
3500	15	182145	59391	253	210282	55319	252
3500	20	182145	71370	184	210282	66835	189

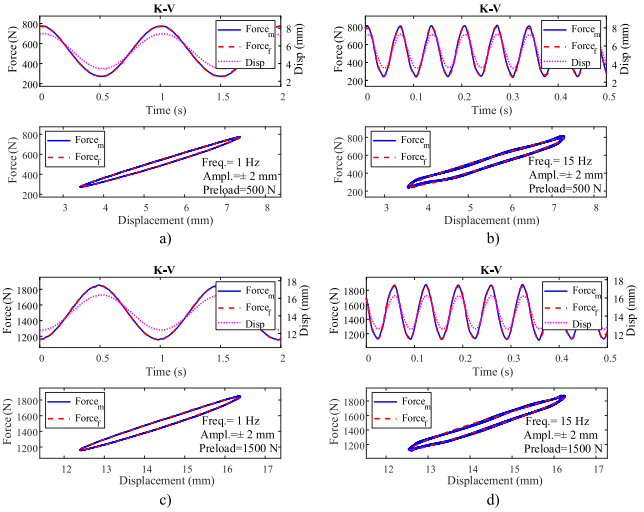

FIGURE 13. Test data fitting using the Kelvin-Voigt model. (a) Frequency 1 Hz, preload 500 N (b) Frequency 15 Hz, preload 500 N (c) Frequency 1 Hz, preload 1500 N (d) Frequency 15 Hz, preload 1500 N.

in Figure 11. This figure has been obtained from tests conducted with a preload of 2500 N, an excitation frequency of 20 Hz, an excitation amplitude of 3 mm and an inflation pressure of 1.8 bar. It can be seen that the three models provided similar results, obtaining error values of the same order in all cases. For comparison purposes, plots include the static stiffness (K_s) measured in the static test. It can be observed that higher dynamic stiffness was obtained compared to the static stiffness. Similar performance was observed in all tests.

5) TIRE INFLATION PRESSURE INFLUENCE

It is well known that static tire stiffness increases with tire inflation pressure. Consequently, for comparative purposes, a second series of tests was carried out with a tire inflation pressure of 2.1 bar and a preload of 3500 N to evaluate its influence on the model parameters. Results are summarized in Table 6. Next, Figure 12 includes the results of this comparison for the Kelvin-Voigt and Maxwell models.

As it can be seen in Figure 12(a) and Table 5, dynamic stiffness decreases when the inflation pressure increases. However, dynamic damping coefficients remain almost independent of the inflation pressure for the Kevin-Voigt model. In contrast, in the Maxwell model, both the dynamic stiffness and damping coefficients are lower when the pressure is increased (see Figure 12b). As expected, Table 6 also shows that static stiffness is higher when the inflation pressure is increased.

B. TESTS WITH A TIRE OF SIZE 90/58 R17

A series of tests was conducted using a 90/58 R17 competition tire. This tire size is commonly used in two-wheeled vehicle races. An amplitude of 2 mm was set in these tests. Test frequencies were 1, 5, 10, 15 and 20Hz. Three preload conditions of 500, 1000 and 1500 N were simulated. Finally, tire inflation pressure was set at 1.9 bar.

1) KELVIN-VOIGT MODEL

The following plots show the results obtained using the Kelvin-Voigt model at two frequencies, 1 and 15 Hz, and preloads of 500 and 1500 N (Figure 13). Plots show the data reproduced by the model according to equations (2) and (3) with the obtained optimized parameters. As in the case of the light passenger car tire, it can be seen that the model reproduced the measured data adequately for all frequencies and preload conditions in all the cases.

Estimated parameters using the Kelvin-Voigt model for all tests carried out with the 90/58 R17 tire are shown in Table 7.

It can be seen in Figure 14 that stiffness and the estimated dynamic damping coefficient have the same behavior as found with the light passenger car tire. That is, stiffness coefficient increases with frequency and damping coefficient decreases towards a low constant value.

TABLE 7. Summary of results using the Kelvin-Voigt model. Tire size: 90/58 R17. Inflation pressure = 1.9 bar.

Preload [N]	Frequency [Hz]	K_s [N/m]	K_d [N/m]	C_d [Ns/m]	Error [N^2]
500	1	101570	21448	2188	6.18
500	5	101570	32100	663	8.30
500	10	101570	36700	366	51.31
500	15	101570	39927	284	155.00
500	20	101570	44430	153	160.12
1000	1	120470	32749	3513	23.95
1000	5	120470	44296	869	43.83
1000	10	120470	50937	361	95.49
1000	15	120470	54038	293	220.46
1000	20	120470	57646	265	213.81
1500	1	142950	35086	3935	19.44
1500	5	142950	49827	941	27.27
1500	10	142950	55839	505	75.05
1500	15	142950	60633	360	200.92
1500	20	142950	65188	306	228.33

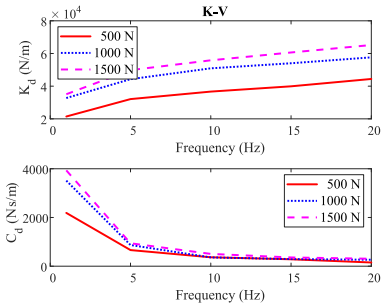

FIGURE 14. Stiffness and damping coefficients of the Kelvin-Voigt model vs excitation frequency. Tire 90/58 R17 (1.9 bar).

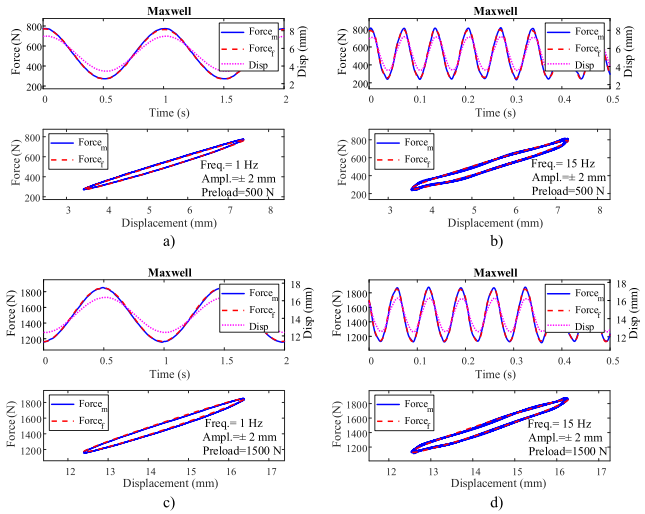

FIGURE 15. Test data fitting using the Maxwell model. (a) Frequency 1 Hz, preload 500 N (b) Frequency 15 Hz, preload 500 N (c) Frequency 1 Hz, preload 1500 N (d) Frequency 15 Hz, preload 1500 N.

2) MAXWELL MODEL

Figure 15 shows the results obtained using the Maxwell model at two frequencies, 1 and 15 Hz and preloads of 500 and 1500 N. The plots show the data reproduced by the model according to equations (2) and (3) with the obtained optimized parameters.

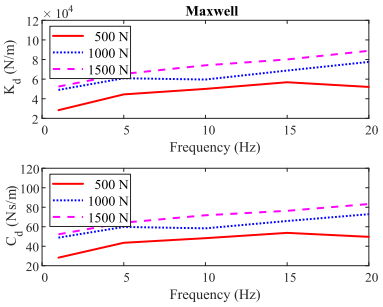

FIGURE 16. Stiffness and damping coefficients of the Maxwell model vs excitation frequency. Tire 90/58 R17 (1.9 bar).

TABLE 8. Summary of results using the Maxwell model. Tire size: 90/58 R17. Inflation pressure = 1.9 bar.

Preload [N]	Frequency [Hz]	K_s [N/m]	K_d [N/m]	C_d [Ns/m]	Error [N^2]
500	1	101570	28369	28.26	93.12
500	5	101570	44431	43.55	165.45
500	10	101570	50049	48.26	93.22
500	15	101570	56850	53.70	222.14
500	20	101570	52052	49.64	260.16
1000	1	120470	49016	48.81	149.36
1000	5	120470	60918	59.79	137.92
1000	10	120470	59601	58.35	352.86
1000	15	120470	68769	65.90	256.71
1000	20	120470	77578	72.88	256.56
1500	1	142950	52458	52.22	305.25
1500	5	142950	65350	64.17	470.01
1500	10	142950	74117	71.77	193.30
1500	15	142950	80090	76.34	147.11
1500	20	142950	88904	83.32	310.10

Table 8 and Figure 16 show the results obtained for the motorcycle tire using the Maxwell model. As before, dynamic stiffness and damping coefficients increase with the excitation frequency increases as well as with the preload.

V. INFLUENCE OF THE TIRE MODEL IN THE VEHICLE VERTICAL DYNAMICS

The influence of the models obtained in the previous section on the behavior of the vehicle suspension system is evaluated next. Most research papers about vehicle vertical dynamics and control algorithms for active and semi-active suspension systems do not take into account the influence of tire damping [20]–[23], or, at best, it is assumed to have a very low constant value [24]–[26]. As shown before, tire damping and tire stiffness depend on the frequency of the excitation. As a consequence, inappropriate modeling of the tire in suspension system models can lead to deterioration in the expected suspension performance [14], [27]. Furthermore, tire stiffness is also modelled with a constant parameter. However, it has also been shown that tire stiffness changes with tire deformation and tire pressure.

The vehicle vertical model shown in Figure 17 was used to evaluate the influence of tire modeling on the performance of the suspension system. K_a and C_a represent suspension stiffness and damping coefficients respectively.

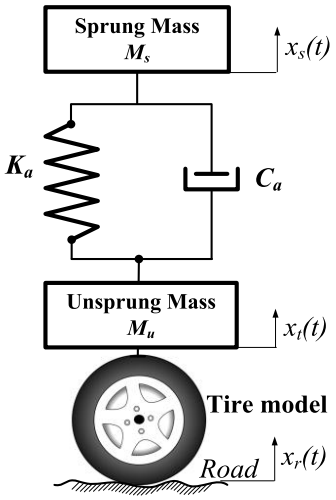

FIGURE 17. Vertical model of a quarter vehicle.

For comparison purposes, the transfer functions of the movement of the sprung mass (H_{SM}), unsprung mass (H_{UM}), sprung mass vertical acceleration (H_A), rattle space (H_{RS}) and tire deflection (H_{TD}) are used. These transfer functions are defined next:

$$H_{SM} = \frac{x_s}{x_r} = \frac{B_1 \cdot B_4}{M_s \cdot s^2 \cdot B_1 + B_2 \cdot B_3} \tag{6}$$

$$H_{UM} = \frac{x_t}{x_r} = \frac{B_2 \cdot B_4}{M_s \cdot s^2 \cdot B_1 + B_2 \cdot B_3} \tag{7}$$

$$H_A = \frac{\ddot{x}_s}{\dot{x}_r} = \frac{B_1 \cdot B_4 \cdot s^2}{M_s \cdot s^2 \cdot B_1 + B_2 \cdot B_3} \tag{8}$$

$$H_{RS} = \frac{x_s - x_t}{\dot{x}_r} = \frac{B_1 \cdot B_4 - B_2 \cdot B_4}{M_s \cdot s^2 \cdot B_1 + B_2 \cdot B_3} \tag{9}$$

$$H_{TD} = \frac{x_t - x_r}{\dot{x}_r} = \frac{B_2 \cdot B_4 - M_s \cdot s^2 \cdot B_1 - B_2 \cdot B_3}{M_s \cdot s^2 \cdot B_1 + B_2 \cdot B_3} \tag{10}$$

where $B_1 = C_a \cdot s + K_a$, $B_2 + M_s \cdot s^2 + C_a \cdot s + K_a$, $B_3 = M_u \cdot s^2 + C_d \cdot s + K_s + K_d$ and $B_4 = C_d \cdot s + K_s + K_d$. Three simulations were performed using the Kelvin-Voigt tire model. The following default parameters were used: $M_s = 250$ kg, $M_u = 35$ kg, $K_a = 16000$ N/m, $C_a = 1600$ N·s/m and $C_d = 170$ N·s/m. In the first simulation, tire stiffness was set at $K_s = 160875$ N/m. This value was obtained from the static test of the car tire with 2500 N of vertical load and a tire pressure of 1.9 bar (see Figure 18, dashed line). In the second simulation, the same parameters were used but tire stiffness was now modelled fitting the data of the previous test to a second order polynomial curve (Figure 18, dash-dottted line). Again, no change in tire stiffness and damping coefficients with the frequency of the excitation were modelled. Finally, in the third simulation, tire damping and stiffness were modelled using the tire model parameters obtained in the test with the car tire with a 2500 N vertical load. In this simulation, both tire damping and stiffness changed with the frequency of the excitation. The following figures show the result of these simulations.

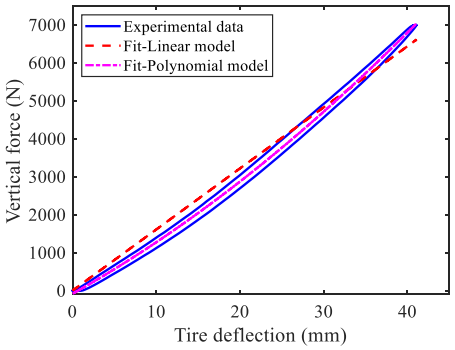

FIGURE 18. Static stiffness. Linear and polynomial fits.

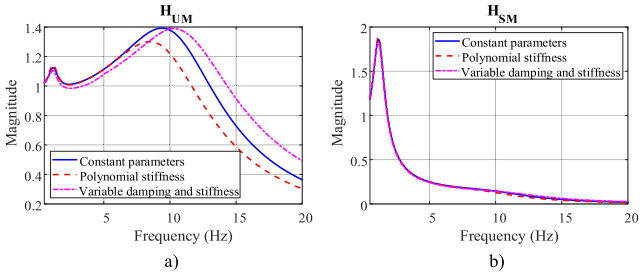

FIGURE 19. Unsprung (a) and sprung (b) masses transfer functions.

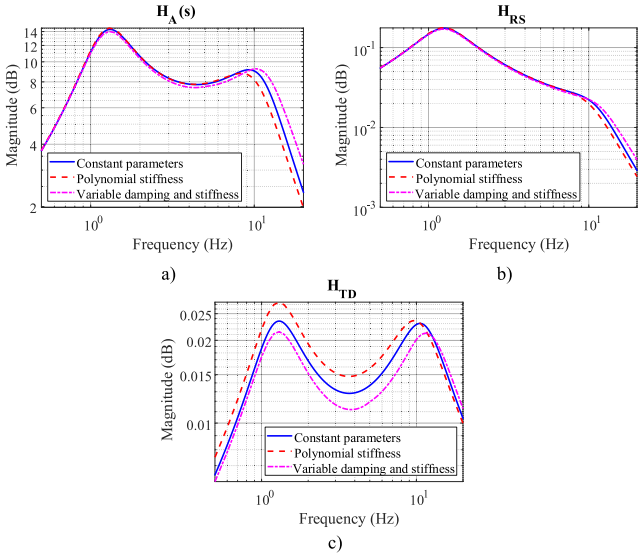

FIGURE 20. Sprung mass acceleration (a), rattle space (b) and tire deflection (c) transfer functions.

As it can be seen in Figure 19a, unsprung mass movement reduces slightly when tire stiffness is not constant (polynomial stiffness) due to the lower tire stiffness in the low range of tire deflections. On the other hand, variable tire stiffness and damping with frequency has a big influence on unsprung mass movement at high frequencies. In addition, the unsprung mass resonant frequency increases due to the increase of tire stiffness with frequency. As a consequence, higher unsprung mass movements are observed at frequencies above the resonant frequency. Sprung mass movement remains almost unaffected with the changes in the parameters (see Figure 19b).

Vertical acceleration and rattle space transfer functions remain almost unmodified no matter if constant or variable static stiffness is used (Figure 20a and 20b). The polynomial stiffness assumption yields lower transfer ratios for frequencies close to and above the unsprung mass resonant frequency while variable damping and stiffness leads to the opposite effect. However, the tire deflection transfer function is remarkably affected by the changes in the parameters. In the first case, it shows higher magnitude levels for frequencies up to the unsprung mass resonant frequency (Figure 20c). On the other hand, the variable damping and stiffness assumption yields lower tire deflections, which is related to lower changes in the tire vertical force and, as a consequence, with better vehicle maneuverability and safety. This way, in this example, the vertical force remains more constant with frequency than expected.

As a summary, it has been demonstrated that the proper modeling of tire stiffness and damping is required to evaluate the performance of vehicle suspension systems and to design vehicle control algorithms. Otherwise, results obtained from simulations can differ significantly from reality.

VI. CONCLUSION

In this paper, the hysteretic and viscoelastic behavior of tires has been evaluated. Three well-known models have been used to reproduce this behavior. To perform this task, model parameters have been obtained from data gathered using a tire test bench using an optimization fitting algorithm. It has been observed that the Kelvin-Voigt and Maxwell lumped models can properly model tire response. The Bouc model yields a slightly better fitting but it requires a higher optimization time and computational cost. The change of model parameters with the frequency of the excitation has been evaluated. It has been demonstrated that tire stiffness and damping coefficients are highly dependent on the frequency of the excitation. Tire stiffness increases with the frequency of the excitation while tire damping is high for low frequencies but it reduces sharply with the increase of frequency. The influence of tire pressure on model parameters has also been studied. It has been shown that as the pressure increases, so does tire stiffness. In this case, little change in tire damping is observed.

Finally, a quarter-car model has been used to evaluate the influence of the previous results on vehicle vertical dynamics. It has been shown that the change of damping and stiffness coefficients with frequency modifies vehicle vertical dynamics. This way, car vertical models should take into account this effect to properly reproduce vehicle movements.

Further works will include a wider range of tires and will focus on new factors, such as excitation amplitude, tire temperature and tire age, related to the determination of tire parameters.

REFERENCES

[1] H. B. Pacejka and I. J. M. Besselink, "Magic formula tyre model with transient properties," *Vehicle Syst. Dyn.*, vol. 27, pp. 234–249, Jan. 1997.
[2] M. Burckhardt, *Fahrwerktechnick: Radschlupf-Regelsysteme*. Würzburg, Germany: Vogel Fachbuch, 1993.
[3] G. Gim and P. E. Nikravesh, "An analytical study of pneumatic tire dynamic properties. Part 1. Pure slips," *Int. J. Vehicle Des.*, vol. 11, no. 6, pp. 589–618, Jan. 1991.
[4] P. Bayle, J. F. Forissier, and S. A. Lafon, "A new tyre model for vehicle dynamics simulations," in *Proc. Automot. Technol. Int.*, vol. 93. London, U.K.: Sterling, 1993, pp. 193–198.
[5] J. Lemaitre, *Handbook of Materials Behavior Models*. Cambridge, MA, USA: Academic, 2001.
[6] A. Hackl, W. Hirschberg, C. Lex, and C. Magele, "Parametrisation of a Maxwell model for transient tyre forces by means of an extended firefly algorithm," *Adv. Mech. Eng.*, vol. 9, pp. 1–11, Oct. 2016.
[7] R. Brancati, S. Strano, and F. Timpone, "An analytical model of dissipated viscous and hysteretic energy due to interaction forces in a pneumatic tire: Theory and experiments," *Mech. Syst. Signal Process.*, vol. 25, no. 7, pp. 2785–2795, Oct. 2011.
[8] Y. Lu, J. Zhang, S. Yang, and Z. Li, "Study on improvement of LuGre dynamical model and its application in vehicle handling dynamics," *J. Mech. Sci. Technol.*, vol. 33, no. 2, pp. 545–558, Feb. 2019.
[9] P. W. A. Zegelaar, "The dynamic response of tyres to brake torque variations and road unevennesses," Ph.D. dissertation, TU DELF, Delft, The Netherlands, 1998.
[10] M. Gipser, "FTire—The tire simulation model for all applications related to vehicle dynamics," *Vehicle Syst. Dyn.*, vol. 45, pp. 139–151, Jan. 2007.
[11] M. Gipser, R. Hofer, and P. Lugner, "Dynamical tyre forces response to road unevennesses," *Vehicle Syst. Dyn.*, vol. 27, pp. 94–108, Jan. 1997.
[12] M. Matsubara, D. Tajiri, T. Ise, and S. Kawamura, "Vibrational response analysis of tires using a three-dimensional flexible ring-based model," *J. Sound Vib.*, vol. 408, pp. 368–382, Nov. 2017.
[13] G. Dihua and F. Chengjian, "Tire modeling for vertical properties including enveloping properties using experimental modal parameters," *Vehicle Syst. Dyn.*, vol. 40, no. 6, pp. 419–433, Dec. 2003.
[14] D. Maher and P. Young, "An insight into linear quarter car model accuracy," *Vehicle Syst. Dyn.*, vol. 49, no. 3, pp. 463–480, Mar. 2011.
[15] D. M. Cuong, S. Sihong, D. V. Hung and N. T. Ngoc, "Study on the vertical stiffness and damping coefficient of tractor tire using semi-empirical model," *J. Sci.*, vol. 83, pp. 5–15, Oct. 2013.
[16] R. K. Taylor, L. L. Bashford, and M. D. Schrock, "Methods for measuring vertical tire stiffness," *Trans. ASAE*, vol. 43, no. 6, pp. 1415–1419, 2000.
[17] Y. Yu, J. Li, Y. Li, S. Li, H. Li, and W. Wang, "Comparative investigation of phenomenological modeling for hysteresis responses of magnetorheological elastomer devices," *Int. J. Mol. Sci.*, vol. 20, no. 13, p. 3216, Jun. 2019.
[18] H. T. Banks, S. Hu, and Z. R. Kenz, "A brief review of elasticity and viscoelasticity for solids," *Adv. Appl. Math. Mech.*, vol. 3, no. 1, pp. 1–51, Feb. 2011.
[19] P. Agarwalla and S. Mukhopadhyay, "Efficient player selection strategy based diversified particle swarm optimization algorithm for global optimization," *Inf. Sci.*, vols. 397–398, pp. 69–90, Aug. 2017.
[20] C. Liu, L. Chen, X. Yang, X. Zhang, and Y. Yang, "General theory of skyhook control and its application to semi-active suspension control strategy design," *IEEE Access*, vol. 7, pp. 101552–101560, Jul. 2019.
[21] M. Z. Q. Chen, Y. Hu, C. Li, and G. Chen, "Performance benefits of using inerter in semiactive suspensions," *IEEE Trans. Control Syst. Technol.*, vol. 23, no. 4, pp. 1571–1577, Jul. 2015.
[22] H. Zhang, Q. Hong, H. Yan, F. Yang, and G. Guo, "Event-based distributed H_∞ filtering networks of 2-DOF quarter-car suspension systems," *IEEE Trans. Ind. Informat.*, vol. 13, no. 1, pp. 312–321, Feb. 2017.
[23] G. Pepe, N. Roveri, and A. Carcaterra, "Experimenting sensors network for innovative optimal control of car suspensions," *Sensors*, vol. 19, no. 14, p. 3062, Jul. 2019.
[24] Y. Huang, J. Na, X. Wu, and G. Gao, "Approximation-free control for vehicle active suspensions with hydraulic actuator," *IEEE Trans. Ind. Electron.*, vol. 65, no. 9, pp. 7258–7267, Sep. 2018.
[25] S. Y. Zhang, M. Zhu, Y. Li, J. Z. Jiang, R. Ficca, M. Czechowicz, R. Neilson, S. A. Neild, and G. Herrmann, "Ride comfort enhancement for passenger vehicles using the structure-immittance approach," *Vehicle Syst. Dyn.*, pp. 1–22, Nov. 2019, doi: 10.1080/00423114.2019.1694158.
[26] W. Xue, K. Li, Q. Chen, and G. Liu, "Mixed FTS/H∞ control of vehicle active suspensions with shock road disturbance," *Vehicle Syst. Dyn.*, vol. 57, no. 6, pp. 841–854, Jun. 2018.
[27] H. Akcay and S. Turkay, "Influence of tire damping on multi-objective control of quarter-car suspensions," in *Proc. IEEE Int. Conf. Ind. Technol.*, Viña del Mar, Chile, Mar. 2010, pp. 100–104.

ENRIQUE CARABIAS ACOSTA received the B.S. and M.S. degrees from the Polytechnic University of Madrid, Spain.

He is currently an Assistant Professor of mechanical engineering with the University of Malaga. His research interests include vehicle dynamics, modeling and control of vehicle safety systems, and parameters estimation.

JUAN J. CASTILLO AGUILAR (Member, IEEE) received the B.S., M.S., and Ph.D. degrees in mechanical engineering from the University of Malaga, Spain.

He is currently an Associate Professor of mechanical engineering with the University of Malaga. His research interests include vehicle dynamics, modeling and control of vehicle safety systems, vehicle testing, optimization algorithms, and parameter estimation.

JUAN A. CABRERA CARRILLO received the B.S. degree in mechanical engineering, the M.S. degree in computer science, and the Ph.D. degree in mechanical engineering from the University of Malaga, Spain.

He is currently a Full Professor of mechanical engineering with the University of Malaga. His research interests include modeling and control of vehicle safety systems and parameter estimation, advanced vehicle systems, genetic algorithms applied to synthesis of mechanisms, tire models and control systems, and spiking neural networks.

JUAN M. VELASCO GARCÍA (Student Member, IEEE) received the B.S. degree in mechanical engineering and electronic engineering, and the M.S. degree in mechatronic engineering from the University of Malaga, Spain.

He is currently a Researcher of mechanical engineering with the University of Malaga. His research interests include vehicle dynamics and parameter estimation.

JAVIER PÉREZ FERNÁNDEZ (Graduate Student Member, IEEE) received the B.S. and M.S. degrees in industrial engineering from the University of Malaga, Spain, where he is currently pursuing the Ph.D. degree in mechanical engineering. He is currently a Researcher of mechanical engineering with the University of Malaga. His research interests include electric vehicles and spiking neural networks.

MANUEL G. ALCÁZAR VARGAS (Student Member, IEEE) the B.S. degree in mechanical engineering and the M.S. degree in industrial engineering from the University of Jaén, Spain. He is currently pursuing the Ph.D. degree in mechanical engineering with the University of Malaga.

He is currently a Researcher of mechanical engineering with the University of Malaga. His research interests include electric vehicles and tire dynamics.